Preparation of VIC Parameters for Findley Lake

Theodore J. Bohn

School of Earth and Space Exploration

Arizona State University

Tempe, AZ, 85287

theodore.bohn@asu.edu

ted.j.bohn@gmail.com

September 25, 2018

Summary

This document describes the derivation of input data for the Variable Infiltration Capacity (VIC) model (Liang et al. 1994) for simulating Findley Lake, WA, USA. This dataset is intended for two purposes: (1) automated testing of the VIC lake module (Bowling and Lettenmaier 2010) within the GitHub and Travis build environment; (2) sample data for users of the VIC model to become familiar with its lake module.

1. Findley Lake

Findley Lake (Fig. 1) is a subalpine lake in the Cascade Mountains, about 65 km east of Seattle, WA, USA. The lake (47.3188 N, -121.5853 E, elevation 1128 m a.s.l.) lies within a cirque of glacial origin, in the headwaters of the Cedar River. Some characteristics of the lake and its catchment are listed in Table 1. Findley Lake was selected for this example for several reasons: (1) it has been studied extensively (albeit in the 1970s and 1980s) by researchers at the University of Washington (Del Moral 1973; Hendrey and Welch 1974; Singer and Ugolini 1976; Tison et al. 1977; Rau 1978; Richey and Wissmar 1979; Richey 1979; Lettenmaier and Richey 1979; Birch et al. 1980; Rau 1980); (2) observations of the complete lake hydrologic budget and various biogeochemical terms have been published and are publicly available; (3) as part of the protected watershed draining into Chester Morse Reservoir, its catchment has experienced very little anthropogenic disturbance in recorded history; (4) land cover within the catchment is fairly homogeneous; (5) the catchment is small enough to fit within a typical VIC grid cell and no major channels feed into the lake, enabling us to establish a control volume corresponding nearly exactly to the lake-catchment system, simplifying our analysis of the model.

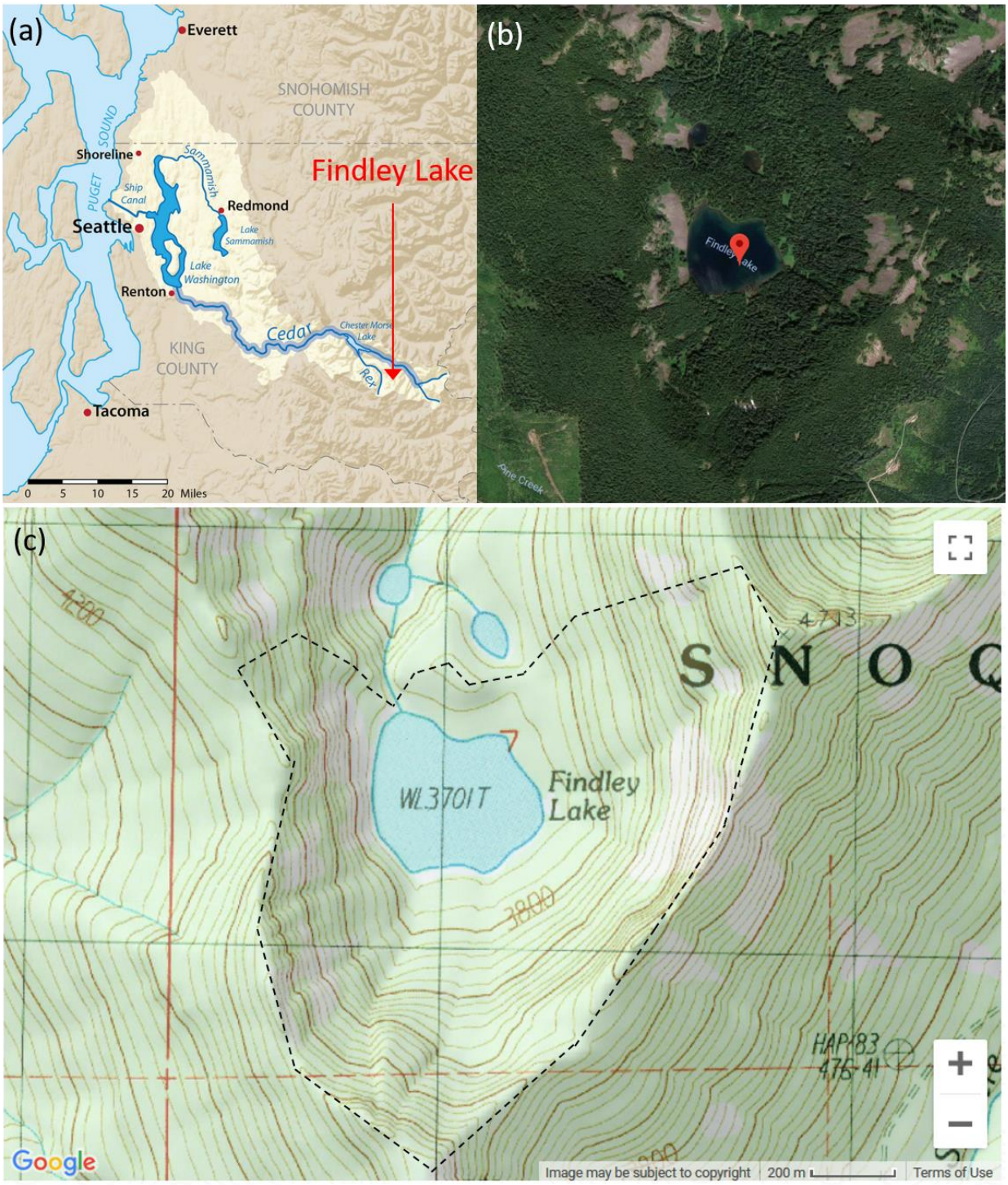

Figure 1. Findley Lake, WA. (a) Location of Findley Lake within the Cedar River Watershed. (b) Satellite imagery of the cirque containing the lake (from Google Maps). (c) Topography surrounding the lake (contour interval = 40 ft) (from https://www.topozone.com). Lake catchment is denoted by dashed line.

Table 1. Key physical properties of Findley Lake.

Parameter	Value	Source
Lake location	(47.3188 N, -121.5853 E)	Estimated here
Lake surface elevation	1128 m	Richey and Wissmar (1979)
Lake surface area	0.114 km^2	Richey and Wissmar (1979)
Spatial maximum depth	27.5 m	Richey and Wissmar (1979)
Spatial average depth	8.7 m	Richey and Wissmar (1979)
Catchment area (including lake)	1.29 km^2	Richey and Wissmar (1979)

2. VIC Model Inputs

In addition to the inputs normally required for VIC model simulations (meteorological forcings and geographic, soil and vegetation parameters), the VIC lake module requires a number of additional lake-specific inputs. The various inputs are summarized in Table 2. Most non-lake inputs were obtained from the MOD-LSP parameter set (Bohn and Vivoni 2019a,b), and either used directly or adjusted. Because the grid resolution of MOD-LSP was 1/16 geographic degrees (6 km), which is much larger than the Findley Lake catchment, values were taken from the single grid cell (47.34375 N, -121.59375 E) that contains the lake.

Table 2. Required inputs to the VIC model. File contents are defined relative to image mode.

File	Category	Variable(s)	Description	Source
Domain	Geography	lat, lon	Coordinates of grid cell centers (decimal degrees)	Estimated here
		elev	Spatial average elevation of cell (m)	Estimated here
		area	Area of cell (m^2)	Estimated here
		mask, frac	Integer and fractional masks indicating which cells fall within basin	MOD-LSP (Bohn and Vivoni 2019a,b)
Forcing	Meteorology	prec, temp, swdown, lwdown, rel_humid, air_pressure, wind	Hourly meteorological fields	Livneh et al. (2015); Bennett et al. (2018); Modified here
Params	Soil	(various) soil properties	Soil physical properties and conceptual parameters	MOD-LSP (Bohn and Vivoni 2019a,b)
	Veg	Cv	Area fractions occupied by land cover classes	Estimated here
		LAI, fcanopy, albedo	Leaf Area Index, canopy fraction, albedo (12 monthly	MOD-LSP (Bohn and

			average climatological values for each land cover class)	Vivoni 2019a,b)
		(various) vegetation properties	Other vegetation structural and phenological parameters	Livneh et al. (2015)
	Snow Bands (optional)	Pfactor, Tfactor, AreaFract	Snow bands parameters	Ignored
	Lake (optional)	lake_idx	Index (within Cv array) of the land cover tile containing the lake	Estimated here
		numnod	Number of nodes (layers) in lake water column	Estimated here
		min_depth	Minimum allowable lake level below which flow in the outlet channel ceases (m)	Estimated here
		wfrac	Ratio of outlet width to lake perimeter	Estimated here
		depth_in	Initial lake depth (m)	Estimated here
		rpercent	Fraction of the surrounding cell surface that drains into lake (fraction of the total runoff and baseflow generated in the cell's other land cover tiles that flows into lake)	Estimated here
		depth-area relationship	Array of (depth,area) pairs defining the lake bathymetry (and topography, when exposed) (m, fraction of grid cell area)	Estimated here

3. Derivation of Inputs Specific to Findley Lake

3.1. Domain file

Geographic and land cover parameters specific to Findley Lake that were not explicitly given in literature (Richey and Wissmar 1979) were derived by visually examining the imagery from Google Maps (Fig. 1b) and topography from TopoZone (https://www.topozone.com) (Fig. 1c) (Table 3). The domain file consisted of a single grid cell, with *lat* and *lon* set to the approximate center of the lake; *area* set to the catchment area (1.29 km^2); *elev* set to the average catchment elevation (1240 m); and *mask* and *frac* each set to 1.

Table 3. Derived and estimated geographic and land cover parameters for Findley Lake.

Parameter	**Value**	**Source**
Average catchment elevation	1240 m	Estimated here

Bare soil area	0.114 km^2	Estimated here
Forest area	1.062 km^2	Estimated here

3.2. Forcings Files

For meteorological fields, daily values of precipitation (*prec*), minimum and maximum air temperature (T_{min}, T_{max}), and wind speed (*wind*) for the period 1974-1975 were taken from the relevant grid cell of the L2015 product. The tool MetSim (Bennett et al. 2018) was used to estimate unobserved variables (*shortwave*, *longwave*, *air_pressure*, *vapor_pressure*) and to disaggregate all variables to an hourly time step using default settings (*prec* disaggregation setting was *uniform*) using the original L2015 grid cell elevation of 989 m. Then, hourly air temperature (*temp*) and *air_pressure* were lapsed to the lake catchment average elevation of 1240 m using a lapse rate of -6.5 K/km and a scale height of 8 km.

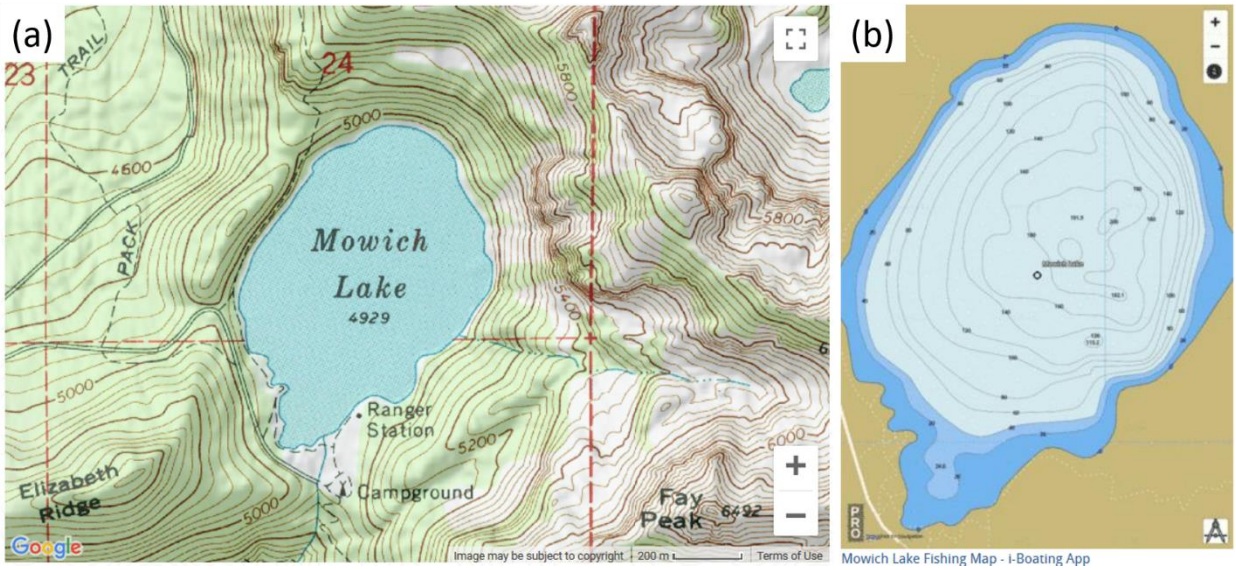

Figure 2. Mowich Lake, in Mt. Rainier National Park, WA. (a) Surrounding topography (contour interval = 40 ft). (b) Lake bathymetry (contour interval = 20 m).

3.3. Params File

Most soil and vegetation parameters were obtained from the relevant grid cell of the MOD-LSP VIC parameter set (Bohn and Vivoni 2019a,b), with values of *lat*, *lon*, and *elev* replaced with those in the domain file. From visual examination of Google Maps imagery (Fig. 1b), land cover class area fractions (stored in the *Cv* array) were assigned manually from the IGBP classification scheme as: "open water" = 0.0885 (= lake surface area / lake catchment area + 0.0001 to allow for potential lake expansion); "bare soil" = 0.0884 (approximately the same area as the lake); and "evergreen needleleaf forest" = 0.8231 (all remaining area within the cell) (Table 3). The open

water class was given the structural properties of bare soil, because the VIC model uses the open water class to represent the behavior of any land surface that is exposed when lake level falls. For evergreen needleleaf forest, the average climatological values of *LAI*, *fcanopy*, and *albedo* given by MOD-LSP were computed from MODIS imagery over the period 2000-2016. Snowband parameters were omitted because this catchment is very so small and values of *elev* only span 300 m. To more accurately reflect the soils in this mountainous domain, the third soil layer thickness was reduced from nearly 2 m to 0.2 m, and the maximum baseflow rate *Dsmax* was reduced from 10 to 1 mm/day (which also helped prevent the lake from draining away).

Lake-specific parameters deal mostly with the spatial configuration of the lake basin. The spatial mean and maximum depths of the lake were provided in literature as 7.8 m and 27.5 m, respectively (Richey and Wissmar 1979). Lacking more detailed information about lake bathymetry, I assumed that the lake basin was approximately bowl-shaped, based on the bathymetry of other lakes found in glacial cirques (e.g., Mowich Lake in Mt. Rainier National Park, WA, Fig. 2). Therefore, following a similar approach to other VIC studies (Bowling and Lettenmaier 2010), I sought to represent bathymetry with a surface of revolution of a polynomial:

$$z(r) = ar^n \quad , \qquad (1)$$

$$A(z) = \pi r^2 = \pi(z/a)^{2/n} \quad , \qquad (2)$$

where *z* is the elevation (m) of the lake basin above its deepest point at distance *r* (m) from the center of the lake; *n* is an integer; *a* is a coefficient for the relationship; and *A(z)* (m^2) is the lake surface area when water level is at elevation *z*.

Assuming the lake is circular, the maximum value of *r* can be computed from surface area A_{surf}:

$$r_{max} = \sqrt{A_{surf}/\pi} = 190m \quad , \qquad (3)$$

The coefficient *a* can be determined by computing the spatial average depth and setting equal to the observed spatial mean depth. First, we compute the spatial average elevation above the lowest point of the surface of revolution $\bar{z}$:

$$\bar{z} = \frac{\int_0^{r_{max}} ar^n 2\pi r dr}{A_{surf}} \quad , \qquad (4)$$

Then, we compute spatial average depth below the surface $\bar{d}$ (observed to be 7.8 m) as:

$$\bar{d} = z_{max} - \bar{z} \quad , \qquad (5)$$

where z_{max} = water elevation above deepest point of the surface of revolution:

$$z_{max} = ar_{max}^n \quad , \qquad (6)$$

Solving for *a*:

$$a = \frac{\bar{d}}{\left(\frac{n}{n+2}\right) r_{max}^n} \quad , \qquad (7)$$

For each integer n from 1 to 5, I computed the parameters of the surface of revolution (Table 4). The best match between z_{max} and the observed maximum depth of 27.5 m occurred for n=1. While the simulated z_{max} of 23.4 m underestimated the observed maximum depth, larger values of n yielded even worse underestimates. Unfortunately, using n=1 resulted in bathymetry that was not particularly bowl-shaped (it is a cone). In addition, the resulting near-shore lake bottom slope was 0.1232, which was much shallower than the average slope of the land surface surrounding the lake (which ranged between 0.3 and 1.0, averaging to about 0.5). Thus, this geometry differs substantially from the geometry of Mowich Lake (Fig. 2). However, Findley Lake is much shallower than Mowich Lake, and if the gradient near-shore bathymetry were similar to that of the surrounding topography, that gradient could not extend far into the lake without overestimating the observed maximum depth and spatial mean depth. Thus, it seems that n=1 is the best choice: it preserves observed storage (by preserving spatial mean depth) and gets close to reproducing observed maximum depth (which constrains bathymetry to have a shallow gradient). The shallow gradient may cause the model to underestimate lake area when lake levels are a few meters below maximum; however I expect this situation to be rare.

Table 4. Parameters of surface of revolution for which r_{max} = 190 m and spatial average depth below surface = 7.8 m.

n	a	$\bar{z}$(m)	z_{max}(m)	Near-shore slope
1	0.1232	15.6	23.4	0.1232
2	4.3213e-4	7.8	15.6	0.1642
3	1.8953e-6	5.2	13.0	0.2053
4	8.9778e-9	3.9	11.7	0.2463
5	4.4102e-11	3.1	10.9	0.2873

The lake depth-area relationship is simply a discretization of Eq. 2, i.e. a discretization of basin shape. I chose to use 9 equally-spaced nodes to sample Eq. 2 at depth intervals of 2.6 m. I created one additional node (for a total of 10 nodes, i.e., *numnod* = 10) at the top to provide a nearly vertical 1-m high wall, to allow the lake level to rise beyond historical levels with minimal impact on lake area. This is somewhat plausible, since lakes often do have small banks along their shorelines. The resulting lake depth-area relationship is given in Table 5 and also plotted in Fig. 3. Note that VIC requires the areas to be expressed as the fraction of total grid cell area (f_{lake}). Furthermore, f_{lake}[0] must equal the area fraction of the land cover tile containing the lake (Cv[“open water”] in this case).

Table 5. Depth-area relationship for Findley Lake.

Element	Elevation above deepest point (m)	Lake surface area (m^2) when water level is at given elevation	Lake surface area / Grid cell area (f_{lake})
0	24.4	114129.0	0.0885
1	23.4	114000.0	0.0884
2	20.8	90074.1	0.0698
3	18.2	68962.7	0.0535
4	15.6	50666.7	0.0393
5	13.0	35185.2	0.0273
6	10.4	22518.5	0.0175
7	7.8	12666.7	0.0098
8	5.2	5629.6	0.0044
9	2.6	1407.4	0.0011
(implied)	0.0	0.0	0.0000

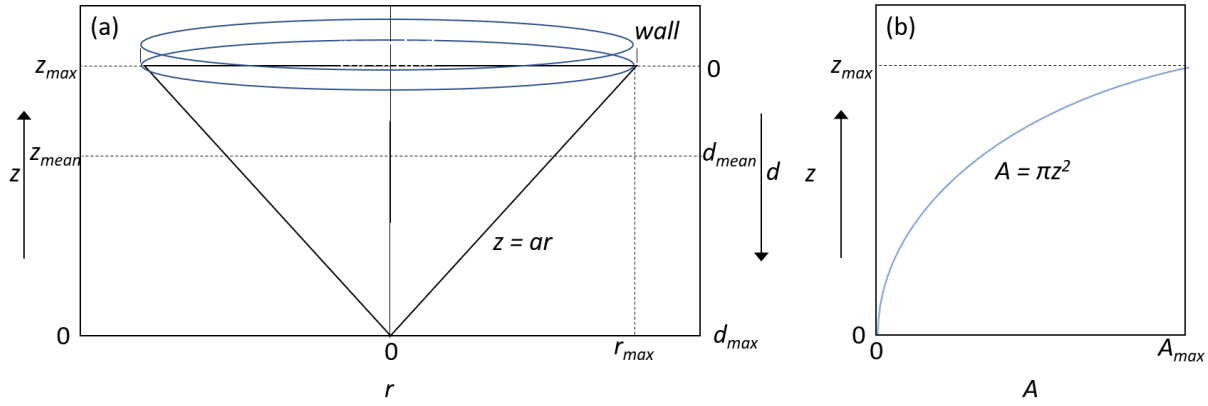

Figure 3. Illustration of depth-area relationship. (a) surface of revolution relating elevation *z* to radius *r*; this is the shape of the lake basin. Depth *d* from surface is plotted on the right-hand y-axis. (b) Relationship between basin area *A* and elevation *z*. Note that the y-axis scale is exaggerated by a factor of 8 relative to x-axis in panel (a); for Findley Lake, z_{max} = 23.4 m and r_{max} = 190 m.

Determining the other lake parameters (Table 6) was fairly straightforward. In the Google Maps imagery (Fig. 1b), the lake outlet (Findley Creek) appeared to be about 2 m wide. Thus, I computed *wfrac* as the ratio of outlet width to lake perimeter:

$$wfrac = \frac{w_{out}}{2\pi r_{max}} \quad , \qquad (7)$$

where w_{out} = outlet width of 2 m.

I assumed the bottom of the outlet channel had the same elevation as the top of the lake basin; thus *min_depth* = 23.4 m. When lake level falls below this elevation, channel outflow ceases. I set the initial lake depth *depth_in* equal to *min_depth*. The lake volume when depth = *min_depth*

is 889,200 m^3. Because I designed the grid cell to correspond exactly to the lake catchment, I assumed that 100% of all runoff and baseflow from the rest of the grid cell flows into the lake; thus *rpercent* = 1.0 (despite its name, *rpercent* is the fraction of runoff and baseflow that flows into the lake, rather than a percent). Finally, I set *lake_idx* equal to 0, indicating that the lake exists in the 0^{th} land cover tile in the cell, namely, the "open water" tile, which occurs first in the list of tiles, i.e., element 0 of the list. Note that the list of tiles I refer to is the list of tiles that have non-zero area in this cell; thus, this list in general contains fewer elements than the *Cv* array, which contains all land cover classes in the classification scheme.

Table 6. Other lake parameters for Findley Lake.

Parameter	Value
numnod	10
wfrac	0.001671
min_depth	23.4 m
depth_in	23.4 m
rpercent	1.0
lake_idx	0

4. Simulations

Simulations were performed with VIC version 5.1.0 (Hamman et al. 2018), using both the "image" (netcdf inputs and outputs) and "classic" (ascii inputs and outputs) drivers. Simulations spanned the period 1970-1979 at 1h time step, with two alternate initial states: 1. a default initial state ("default"); and 2. an initial state set to the model state at the end of 1979 in the "default" simulation ("with_spinup").

Observed fluxes (Richey and Wissmar 1979) were reported at seasonal intervals over the period 1974-1975, although the exact beginning and ending dates of these seasons were not given. Simulated fluxes were aggregated to the seasonal scale ("winter" = January-March; "spring" = April-June; "summer" = July-September; "fall" = October-December) for comparison. Observed fluxes were reported as volumes and grouped into the following terms: fluvial inflow, precipitation over the lake, total outflow, evaporation over the lake, and change in lake water storage. For comparison, the VIC outputs were combined as follows: fluvial inflow = OUT_LAKE_RO_IN_V + OUT_LAKE_BF_IN_V; precipitation over the lake = OUT_LAKE_PREC_V; total outflow = OUT_LAKE_CHAN_OUT_V + OUT_LAKE_BF_OUT_V; evaporation over the lake = OUT_LAKE_EVAP_V; change in storage = OUT_LAKE_DSTOR_V + OUT_LAKE_DSWE_V.

5. Results and Discussion

The "default" and "with_spinup" simulations were essentially identical after the first year of simulation (which implies a surprisingly short "memory" for this system). Therefore, I'm only showing the "default" results hereafter.

Fig. 4 depicts observed and simulated seasonal water balance terms for the period 1974-1975. Inflow and outflow were the dominant terms in both the observed and simulated lake water budgets. For inflow (Q_{in}), outflow (Q_{out}), and P over the lake, simulated and observed terms were approximately the same order of magnitude, and the match was good for 1975. However, for 1974, simulated Q_{in} differed substantially from observed. Simulated Q_{in} is generated outside the lake module and reflects the water balance in the surrounding catchment. For *ET*, the match was not particularly good in either year. However, the "observed" term was actually potential *ET* computed from meteorology, and apparently did not account for the presence of lake ice, so we should not place much importance on mismatches here. Furthermore, both simulated and observed *ET* were much smaller than the other fluxes, so that discrepancies in *ET* played only a small role in the water budget.

Observed and simulated change in storage (ΔS) had the worst (relative) discrepancies of all terms, with simulated changes over 10 times the size of observed changes and often in the opposite direction. However, even simulated ΔS was 1/20 the size of Q_{in} and Q_{out}, so that discrepancies between simulated and observed values played only a minor role in the water budget. Still, the larger amplitude of simulated ΔS implies that either (a) the chosen value of *wfrac* is too small or (b) baseflow out of the lake is too small (however, baseflow out of the lake is linked to baseflow into the lake in the current model, making adjustment of baseflow problematic).

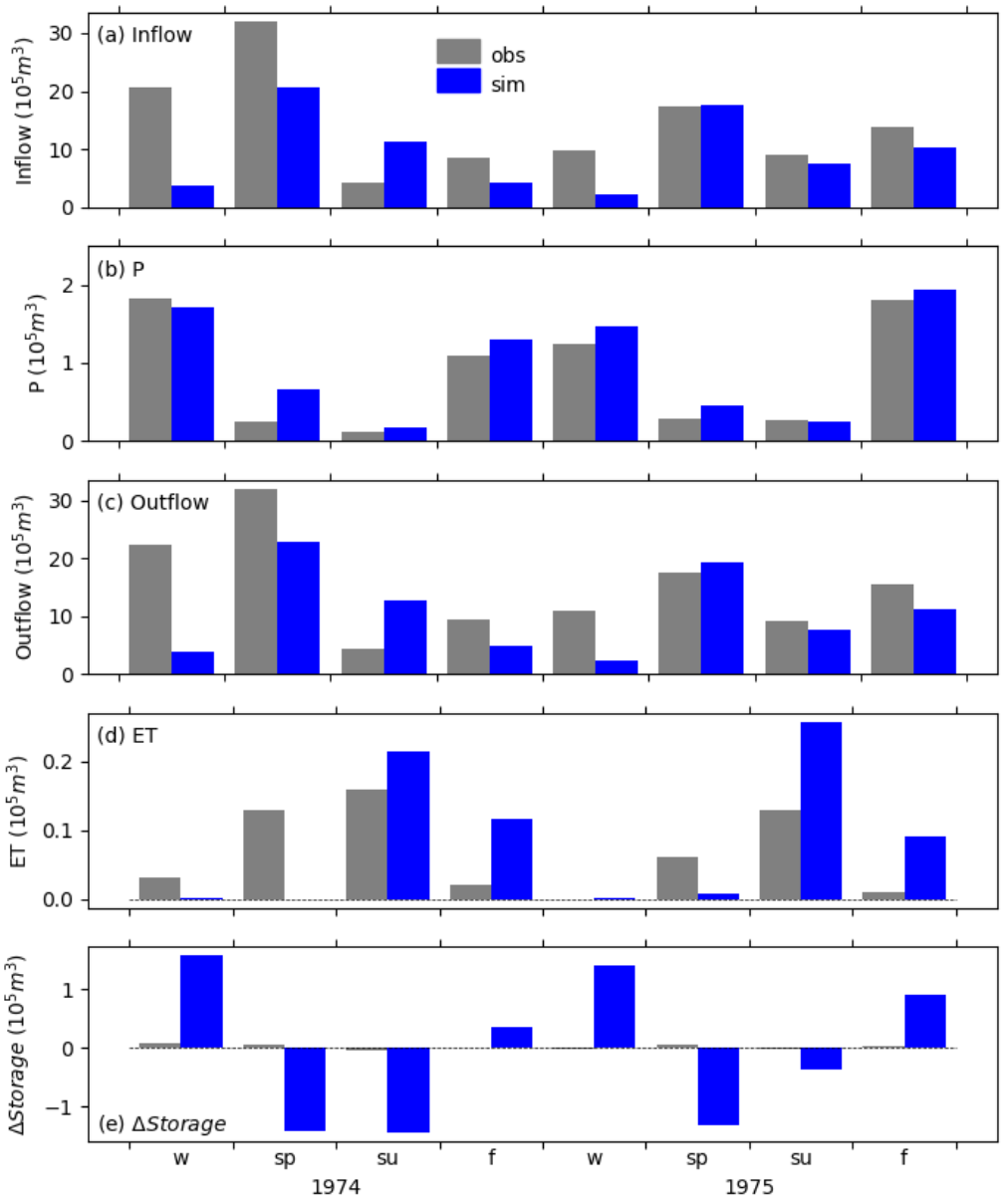

Figure 4. Observed and simulated seasonal water balance terms at Findley Lake over the period 1974-1975.

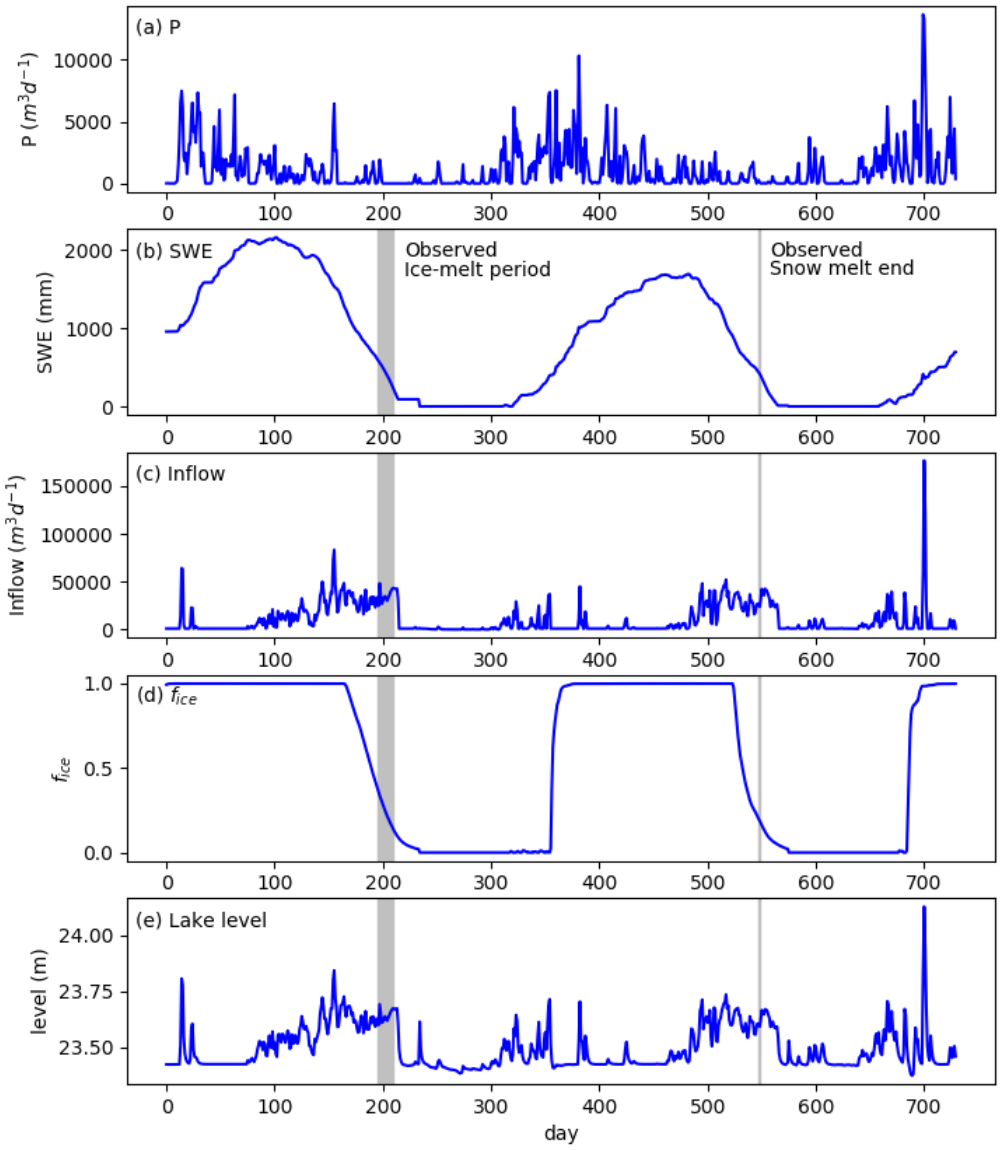

Figure 5. Simulated hydrologic terms at daily resolution for Findley Lake, 1974-1975. The observed ice-melt period in 1974 and date of the end of snow melt in 1975 are denoted in gray.

Fig. 5 shows simulated hydrologic terms at daily resolution for the period 1974-1975. Precipitation from the L2015 product (Fig. 5a) matches the description in literature (Richey and Wissmar 1979). Simulated snow melt in 1975 was mostly complete by the recorded snow-free

date (July 1) for that year, but still continued for another two weeks (Fig. 5b). This suggests that the simulated snow melt was too slow or started too late. The ice-covered fraction of the lake surface f_{ice} was declining during the 2-week period of ice decline reported in the literature, but began well before and continued well after, suggesting that the ice melt rate in the lake model is too slow (Fig. 5d). The simulated lake level (Fig. 5e) was highly correlated with lake inflow (Fig. 5c), which can be attributed to (1) inflow and outflow being the largest terms in the water budget and (2) lake residence time being short, so that there is little lag between changes in inflow and lake level. A longer residence time, which could be achieved by a smaller outlet width *wfrac* (and requiring a taller wall at the top of the lake basin) would create noticeable lags between inflow and lake level, as well as larger amplitude variability in lake level. However, as noted earlier, *wfrac* is likely too small.

To improve the fit with observations, I've listed a few possible strategies in Table 7.

Table 7. Potential strategies to employ for improving model fit to observations.

Symptom	**Potential Remedies**
Large amplitude of changes in storage	• Increase outlet width (*wfrac*). If *wfrac* is too small, channel outflows will be too slow, and lake level will rise too much in response to an inflow pulse. If we were to plot fluxes at the hourly scale, we might also see a small recession in lake level and outflow after each inflow pulse. Increasing *wfrac* will reduce the length of time of the recession as well as reducing the amplitude of lake level fluctuations. • In general, we can reduce the amplitude of storage changes by reducing max baseflow rate (*Dsmax*), although in this case I've already reduced *Dsmax* and further reduction is unlikely to have much impact. However, in the current model, modifying *Dsmax* can be problematic (see "Recommended Model Changes" below).
Mismatches in winter inflow	• Modify snow model behavior: rain/snow transition temperatures, snow albedo parameters, possibly modify the model to have more snow layers. For example, simulated inflow during winter of 1974 was much smaller than observed, implying a potential problem in rain/snow partitioning. Another example: the snow melt period extended later into the season than observed in 1975, so either the pack was too large or it melted too slowly, or both. In addition, parameters that might impact the rates of snow sublimation and evaporation of melt water could impact the amount and rate of snow melt. • Try turning on snow bands. This would allow us to have the lake at warmer lower elevation, along with part of the surrounding uplands with less snow, and a colder upper elevation with more snow. Unfortunately, to do this would require changes to the current model (see "Recommended Model Changes").

Mismatches in spring-fall inflow	• Modify upland soil parameters: third layer *depth*, b_{infilt}, *Ds*, *Ws*, *Dsmax*. What is needed is to change the partitioning of *P* (which appears to match observations fairly well) into *ET*, *Q*, and changes in soil moisture storage. Unfortunately, modifying upland soil parameters, particularly *Dsmax*, will impact the rate of baseflow out of the lake (see "Recommended Model Changes").

Recommended Model Changes

Finally, here are a few model improvements that I recommend:

- **Add lake water temperature profile output variable.** The current model does not have a variable available to report the lake water column temperature profile. Observations do exist of water temperatures in Findley Lake (Richey and Wissmar 1979). Comparison of simulated and observed temperature profiles would help evaluate the physics of lake mixing and heat transfer. These, in turn, could influence the timing of ice cover, the breakup of which began earlier in the simulations than reported.
- **Allow the lake-bottom soil to have a different value of maximum baseflow rate *Dsmax* than the rest of the grid cell.** In the current model version (5.1.0), all soils in the grid cell have the same value of *Dsmax*. This is problematic because baseflow from the rest of the grid cell is an input to the lake, while baseflow from the lake bottom is an outflow. Thus, a user currently does not have the ability to calibrate lake inflows and outflows independently. In reality, lake-bottom soils can be quite different from the surrounding uplands, in both layer thickness and soil texture. In addition, lake-bottom soils are continuously saturated, while upland soils are rarely saturated. In the model, saturated lake-bottom soils will generate baseflow at the maximum rate (*Dsmax*) but upland soils generally generate far lower rates of baseflow, such that the typical practice of calibrating soil parameters of an entire river basin to match observed streamflow will (a) not be sensitive to the value of *Dsmax* and (b) yield an optimal value of *Dsmax* that may not be optimal for lake-bottom soils.
- **Enable snow bands and lakes to exist simultaneously.** In the current model version (5.1.0), snow bands and lakes cannot be turned on simultaneously due to assumptions each feature makes about land cover tiles and snow bands. Furthermore, if someone were to fix that problem, the code would place an identical lake in every snow band, which certainly does not accurately represent the Findley Lake case. Thus, ideally, the model should allow each snow band to have a distinct lake area (which might be 0 in many cases).

References

Bennett, A., J. J. Hamman, B. Nijssen, E. A. Clark, and K. M. Andreadis, 2018: UW-Hydro/MetSim: Version 1.1.0 (version 1.1.0). *Zenodo*, doi:10.5281/zenodo.1256120. http://doi.org/10.5281/zenodo.1256120 (Accessed June 7, 2018).

Birch, P. B., R. S. Barnes, and D. E. Spyridakis, 1980: Recent sedimentation and its relationship with primary productivity in four western Washington lakes 1. *Limnol. Oceanogr.*, **25**, 240–247.

Bohn, T. J., and E. R. Vivoni, 2019a: MOD-LSP, MODIS-based parameters for hydrologic modeling of North American land cover change. *Nat. Sci. Data*, **(submitted)**.

——, and ——, 2019b: MOD-LSP: MODIS-Based Parameters for Variable Infiltration Capacity (VIC) Model over the Continental US, Mexico, and Southern Canada (Version 1.0) [Data set]. *Zenodo*, doi:10.5281/zenodo.2612560. https://zenodo.org/record/2612560.

Bowling, L. C., and D. P. Lettenmaier, 2010: Modeling the effects of lakes and wetlands on the water balance of Arctic environments. *J. Hydrometeorol.*, **11**, 276–295.

Del Moral, R., 1973: The vegetation of Findley Lake basin. *Am. Midl. Nat.*, 26–40.

Hamman, J. J., B. Nijssen, T. J. Bohn, D. R. Gergel, and Y. Mao, 2018: The Variable Infiltration Capacity Model, Version 5 (VIC-5): Infrastructure improvements for new applications and reproducibility. *Geosci. Model Dev.*, **11**, 3481–3496.

Hendrey, G. R., and E. B. Welch, 1974: Phytoplankton productivity in Findley Lake. *Hydrobiologia*, **45**, 45–62.

Lettenmaier, D. P., and J. E. Richey, 1979: Use of first-order analysis in estimating mass balance errors and planning sampling activities. *Theoretical Systems Ecology*, Elsevier, 79–104.

Liang, X., D. P. Lettenmaier, E. F. Wood, and S. J. Burges, 1994: A simple hydrologically based model of land surface water and energy fluxes for general circulation models. *J. Geophys. Res. Atmospheres*, **99**, 14415–14428.

Rau, G., 1978: Carbon-13 depletion in a subalpine lake: carbon flow implications. *Science*, **201**, 901–902.

Rau, G. H., 1980: Carbon-13/carbon-12 variation in subalpine lake aquatic insects: food source implications. *Can. J. Fish. Aquat. Sci.*, **37**, 742–746.

Richey, J. E., 1979: Patterns of phosphorus supply and utilization in Lake Washington and Findley Lake 1, 2. *Limnol. Oceanogr.*, **24**, 906–916.

——, and R. C. Wissmar, 1979: Sources and influences of allochthonous inputs on the productivity of a subalpine lake. *Ecology*, **60**, 318–328.

Singer, M. J., and F. Ugolini, 1976: Hydrophobicity in the soils of Findley Lake, Washington. *For. Sci.*, **22**, 54–58.

Tison, D. L., F. E. Palmer, and J. T. Staley, 1977: Nitrogen fixation in lakes of the Lake Washington drainage basin. *Water Res.*, **11**, 843–847.